ELSEVIER

Nuclear Instruments and Methods in Physics Research A 432 (1999) 364–373

NUCLEAR INSTRUMENTS & METHODS IN PHYSICS RESEARCH Section A

www.elsevier.nl/locate/nima

Measurements of photomultiplier single photon counting efficiency for the Sudbury Neutrino Observatory

S.D. Biller[a], N.A. Jelley[a], M.D. Thorman[a,*], N.P. Fox[b], T.H. Ward[b]

[a]*Nuclear and Astrophysics Laboratory, University of Oxford, Keble Road, Oxford, OX1 3RH, UK*
[b]*National Physical Laboratory, Teddington, Middlesex, TW11 0LW, UK*

Received 11 February 1999

Abstract

A knowledge of the absolute efficiency of the photomultiplier tubes (PMTs) used in the Sudbury Neutrino Observatory (SNO) is important for modelling the behaviour of the detector. While the quantum efficiencies for the PMTs are known, the efficiency in single-photon counting mode (which includes collection efficiency and counting efficiency) is of more relevance. A calibration of the 8 in. Hamamatsu R1408 photomultipliers in this mode requires a known flux of incident light at the very low level of 10^{-16} W cm^{-2} (250 photons cm^{-2} s^{-1}). A method of performing such measurements, utilising the extreme linearity obtainable with silicon photodiodes, is presented in this paper. The results of efficiency measurements on four PMTs are given and a comparison is made with previous results obtained using a Cherenkov source of known intensity.

PACS: 85.60.Ha; 26.65. + t

Keywords: Photomultiplier absolute efficiency; Single-photon counting; Solar neutrinos; Cherenkov sources

1. Introduction

The Sudbury Neutrino Observatory (SNO) [1] is a 1000 tonne heavy water Cherenkov detector situated at a depth of 6800 ft in INCO's Creighton mine at Sudbury, Canada. Its primary purpose is to observe interactions of neutrinos from the sun in an attempt to test the hypothesis of neutrino oscillations as the origin of the observed deficiency in solar neutrinos (the Solar Neutrino Problem). The detector employs an approximately spherical array of ~9500 Hamamatsu R1408 8 in. photomultiplier tubes (PMTs) which will be used to observe the Cherenkov light produced as a result of neutrino interactions occurring within an inner volume of heavy water.

An a priori knowledge of the absolute PMT efficiency as a function of wavelength is important in modelling the response of the detector and in investigating systematic detector effects with detailed Monte Carlo calculations. Given information on light attenuation in the detector, it allows a prediction of the energy response to be made, i.e. the number of Cherenkov photons observed from an electron of a given energy. This would serve as

* Corresponding author. Tel.: + 44-1865-273442; fax: + 44-1865-273418.

E-mail address: m.thorman1@physics.ox.ac.uk (M.D. Thorman)

0168-9002/99/$ - see front matter
PII: S0168-9002(99)00500-8

a valuable cross-check with the in situ methods of calibration using beta-decay sources such as ^{16}N.

If the photomultipliers had perfect photoelectron collection then their efficiency would be equivalent to their quantum efficiency, which is widely quoted by manufacturers. This quantity is measured relatively straightforwardly by connecting up the PMT as a diode so that the whole dynode stack is held at the same potential. Any photoelectrons produced will all contribute to an anode current which can be measured at high illumination without risk of damaging the PMT. However, with the PMT operating in single-photon counting mode, one must include the efficiency for collection of photoelectrons on the first dynode, and the probability that the subsequent charge pulse will exceed the discriminator threshold in the associated electronics (the counting efficiency).

The problem with measurements of the photon counting efficiency is that a very low light level is required. This could be obtained with a calibrated light source of sufficiently low intensity or by attenuating a measured beam by an accurately known amount. Measurements on a Hamamatsu PMT of the type used in SNO have been made by Boardman et al. who constructed a Cherenkov source [5] of sufficiently low intensity for single-photon counting. This required accurate measurements of the activity of the source and detailed Monte Carlo calculations of the energy loss and Cherenkov light production. An uncertainty of 3.5% was quoted for the source intensity. The wavelength dependence had to be taken from quantum efficiency measurements.

For the measurements described here, a more direct approach was adopted which took advantage of the extreme linearity obtainable with silicon photodiodes. The method involved focussing a monochromatic beam into an integrating sphere which had one exit port providing illumination for the PMT under test while the light level was continuously monitored by a photodiode in close proximity to a second port. At a sufficiently high intensity, the absolute flux of light incident on the PMT was determined with a second photodiode of known absolute efficiency as a function of wavelength (ultimately calibrated against a cryogenic radiometer). The necessary reduction in intensity required for single-photon counting measurements was achieved with neutral density filters placed before the integrating sphere. It was not necessary to know the attenuation of the filters as this was accurately determined from the change in output of the monitor photodiode.

This arrangement enabled a precise calibration over the complete range of wavelengths of interest. The PMTs were fitted with SNO base circuitry and the electronics were configured to model those in the actual SNO detector with the discriminator level set at $\frac{1}{4}$ of a single photoelectron (this will later be defined more precisely). The same area of the PMT photocathode was exposed as in the actual detector but no light concentrator [2] was attached and the incident light was directed in a nearly parallel beam along the axis of the PMT. Typical count rates of 10^4 Hz were used for the measurements.

The results of the efficiency measurements can, in a sense, be used as a normalization in the modelling of the SNO photomultiplier tubes. Previous work [3,4] has shown that the PMT response can be well described by a full geometrical model of the optics and a detection probability for photons striking the photocathode given by

$$P = A(\lambda, \theta) P_{\mathrm{esc}}(\lambda)\, \eta_{\mathrm{c}} \tag{1}$$

where A is the absorption, P_{esc} the probability that a photoelectron escapes from the photocathode, and η_{c} the collection efficiency. The absorption in the photocathode, A, can be calculated from Fresnel's laws applied to a material with complex refractive index, and by taking into account the interference between multiple reflections within the photocathode itself. The model may be used to calculate the average probability of photons being absorbed in the photocathode, given that they are incident on the PMT in the particular geometry used in our efficiency measurements. By comparing this with the actual measured efficiency, the product $P_{\mathrm{esc}}(\lambda)\eta_{\mathrm{c}}$ in Eq. (1) may be obtained. This provides a wavelength-dependent normalization for subsequent calculations of the response to light in new geometries. In particular, if a parallel rather than diverging beam were used in our measurements, the efficiency is expected to increase by a factor of 1.004. The SNO light concentrators increase

the collection area by 75% [2], and along with the effect of immersing the PMT in water, change the angles at which light is incident on the photocathode. For photons originating from all regions of the SNO detector, the average probability of detection of those that make it to the PMT is predicted to be greater than our measured value by a factor $\sim$1.1 at 420 nm.

The measurements were carried out at the National Physical Laboratory in the UK with photomultiplier tubes and associated electronics provided by SNO. Four PMTs were measured in all, three of which were later to be placed in the detector (serial codes PPNY, PPOZ, PAVJ). The fourth PMT (serial code CB0274) was the same one used by Boardman et al. [5] for calibration with the Cherenkov source, and allowed a comparison of the two techniques.

2. Description of the system

2.1. Calibrated light source

Fig. 1 shows the experimental arrangement. The system was designed to illuminate a photomultiplier tube with an approximately uniform beam of depolarised radiation of known intensity and spectral content. The light source was either a tungsten strip lamp or high-pressure xenon arc. The tungsten lamp was used initially for short wavelengths but the xenon arc was found to be adequate over the full range in later measurements.

The light from the source was passed through a double-grating monochromator which offered good rejection of stray light. In addition, the photodiodes have no sensitivity above 1.2 μm so the measurements will not be affected by any stray light at longer wavelengths, where the source output is high. The gratings of the monochromator were optimised for the ultra-violet and visible regions of the spectrum. Second-order filters were used to prevent the transmission of wavelengths from the second order of the gratings. This provided monochromatic light with a bandwidth of 6.5 nm FWHM.

The beam could then be passed through optional apertures and neutral density filters allowing the intensity to be reduced by a factor of up to 10^3 before entering the first light exclusion box. A shutter was included to block the beam for measurements of the dark count rate. Inside this box, the beam was focussed into a 50 mm diameter integrating sphere which acted as a diffuser, improving the uniformity of the radiation, providing further attenuation (another factor of $\sim 10^3$) and depolarisation. The sphere had two exit ports at right-angles to the entrance port, both 5 mm in diameter. One port was monitored by a silicon photodiode (Hamamatsu 1227) attached to a low-noise amplifier. The second opened into a separate light exclusion box and provided illumination for the PMT

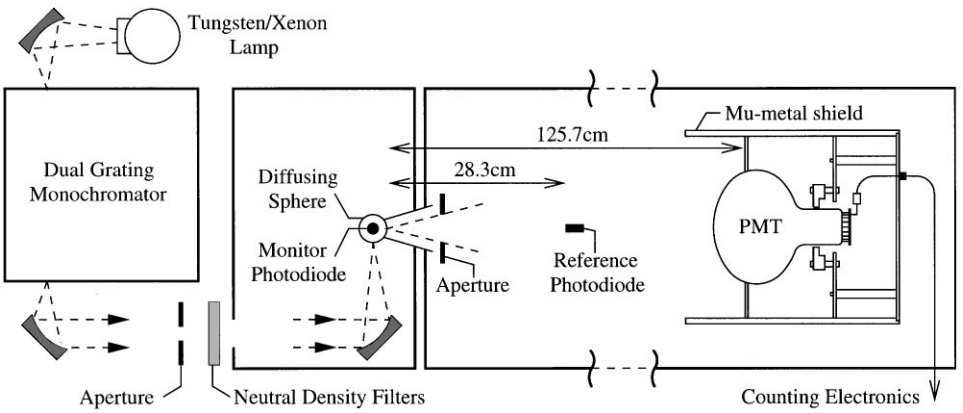

Fig. 1. A schematic diagram of the system used for measuring PMT photon-counting efficiency.

under test. The precise location of the light source was defined by the plane of a 1 mm diameter, blackened, chamfered aperture, placed in front of the port. The opening angle was limited by a larger aperture so that the field did not extend significantly beyond the edge of the PMT housing. This prevented light from being directly scattered onto the PMT from the walls of the box.

The integrating sphere was coated internally with a barium sulphate paint which is known to have good lambertian properties and is reasonably stable in time. For the purpose of this measurement the sphere needed to be stable during the time between its initial calibration and that of the PMT (typically a few days). This is well within the capabilities of the sphere and in fact, since the calibration procedure required it to be calibrated both before and after the PMT, any drift would be observed and could be accounted for (none was observable within the uncertainty of our measurements).

The flux of light per unit solid angle from the exit port varied as $\cos\theta$, where θ is the angle from the optical axis. To a good approximation, the light is therefore uniform over the solid angle of the PMT. This was checked by taking measurements with a separate one inch PMT in this plane. No variation was observed at the 1% level.

At various stages of measurement, the absolute flux from the exit port was measured with a second silicon photodiode (1 cm^2 Hamamatsu 1227) calibrated in W cm^{-2} against NPL standards for spectral responsivity. For wavelengths above 400 nm, the scale is set by the NPLs primary standard cryogenic radiometer which makes use of the equivalence of optical and electrical heating (see for example Ref. [7]). Such calibrations are carried out at the 0.5 mW level with a series of laser lines. The extreme linearity of silicon photodiode devices is then used to allow extrapolation down to the power levels used in this measurement (1 pW). Linearities are demonstrated (also discussed in Ref. [7]) by dividing a beam into two components and comparing the sum of the photocurrent for each beam individually to that for the combined beam. This is repeated as many times as necessary, each time halving the intensity of the beams. The degree of non-linearity of a Hamamatsu S1337 is reported in Ref. [7] to be better than 10^{-4} over five orders of magnitude in radiant power. At wavelengths shorter than 400 nm, the photodiodes are calibrated by extrapolation of visible calibrations using spectrally flat or black detectors. These black detectors are usually thermal in nature and thus have poorer noise performance than the solid-state detectors used in the visible and thus the responsivity is therefore known less accurately [9].

The light level could not be made sufficiently high to permit a measurement with the reference photodiode at the PMT position (the limit being imposed by the noise level of the photodiode). However, a measurement of flux per steradian could be made closer to the integrating sphere so that the total flux on the PMT could be inferred from the known solid angle it covered. The precise distance from the reference photodiode to the exit port of the sphere was determined by making measurements in several positions, and performing a fit to an inverse-square law (with the light source replaced by a laser for the convenience of measuring fluxes at higher levels). The data were consistent with a distance of 28.3 ± 0.1 cm for the reference detector.

Before measuring count rates with the PMT at the level of 10,000 Hz, the beam had to be further attenuated by introducing the neutral density filters. The reduction in flux from the exit port of the integrating sphere was inferred from the change in the output of the monitor photodiode, relying on the photodiode linearity.

2.2. Photomultiplier tube and housing

As each of the PMTs were tested, they were mounted with their front face aligned perpendicularly to the optical axis and facing the exit port of the integrating sphere. The PMT housing consisted of an aluminium-walled cylindrical can, open at one end. This was wrapped in μ-metal sheets to provide screening from the earth's magnetic field. The residual field inside the housing was measured as 3 μT, which was estimated to lower the efficiency by a factor 0.996 ± 0.002 based on the results of previous work [8]. The measured efficiencies have been corrected for this.

The PMT was held firmly against a defining aperture mounted 10 cm behind the open face of

the can. The diameter of the aperture was 196.82 ± 0.05 mm, exposing an area of photocathode equal to that of the PMTs in the SNO detector. The distance of the plane of the aperture from the source was directly measured to be 125.7 ± 0.1 cm.

The defining aperture was made from a matt black material, and the exposed inner walls of the can in front of the aperture were clad with a rough black material to minimise any contribution to the signal from scattered light. The residual amount of scattering was determined in a separate measurement by simply blocking the direct light from a source and measuring a count rate above the dark level. This gave a value of $(0.50 \pm 0.05)\%$ which was subtracted from measurements.

The four PMTs tested were wired with a standard SNO base as shown in Fig. 2. A single co-axial cable carries both the signal and high voltage. Good grounding of the cable to the metal can ensured minimal RF pickup.

2.3. Counting electronics

A schematic diagram of the counting electronics associated with the PMT is shown in Fig. 3. The PMTs were operated at typical voltages of 1900 V in order to achieve a gain of 10^7, the specification for the SNO experiment. Note that half of the charge is lost via the 75 Ω PMT base termination so the actual gain seen by the electronics was lower. The signal was extracted from the high-voltage line with a simple RC filter circuit and then amplified by a factor of 40 using a LeCroy 612A unit. One amplifier output was connected to a fast discriminator which generated a 64 ns long pulse to provide a gate for a LeCroy 3001 'qVt' multichannel analyser (MCA) and an input to a scaler. The scaler had a second input which was clocked at 1 MHz to provide an accurate means of measuring time intervals for pulse counting.

A second amplifier output was connected to the charge input of the MCA after passing through a suitable delay (~ 32 ns). The MCA recorded a charge spectrum which could be used to set the discriminator level to $\frac{1}{4}$ spe (single photoelectron). An example is shown in Fig. 4. The spe was defined as the charge q such that the mean of the charge spectrum in the range $0.25q$–$2.5q$ was precisely q. This uniquely defined a discriminator setting for the determination of absolute efficiency. In practice, it was not necessary to set this exactly as

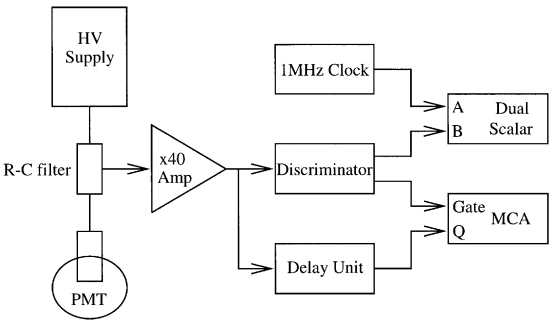

Fig. 3. The counting electronics.

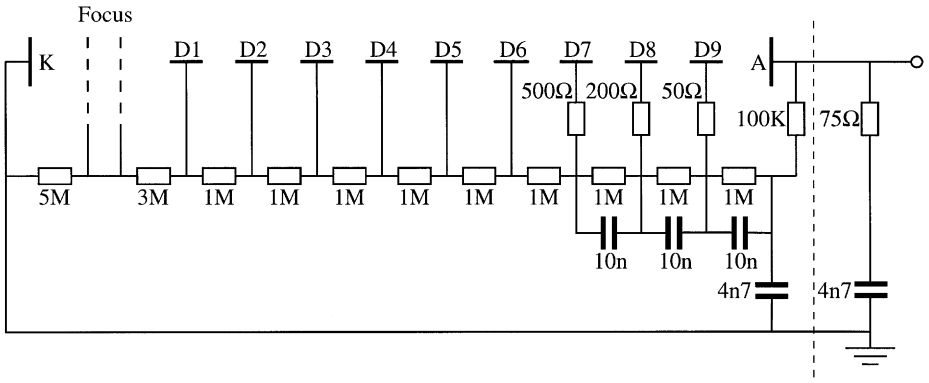

Fig. 2. The SNO PMT base circuit.

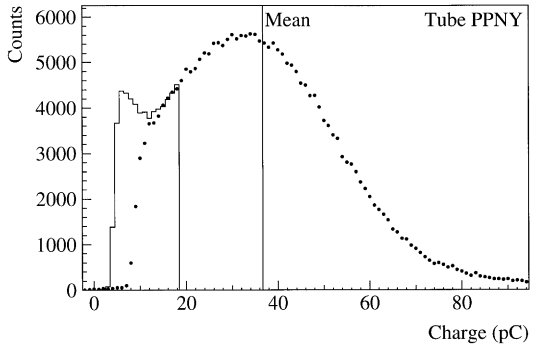

Fig. 4. A charge spectrum from PPNY. The mean (as defined in the text) is shown, and the discriminator edge lies at approximately $\frac{1}{4}$ of this. Also shown (solid histogram) is a portion of a spectrum with the same normalization and taken with a lower discriminator setting, revealing the 'valley' in the distribution. This feature is less pronounced in CB0274 and PAVJ.

a small correction to the count rate could be made based on the known shape of the charge spectrum. Approximately 8% of the spectrum lies above $2.5q$ and 14% below $0.25q$, the latter being a more uncertain estimate since it requires extrapolation below the lowest point at which the discriminator level could be set (~ 0.1 spe).

2.4. Afterpulsing

The count rate measured from a PMT will include a contribution from after-pulsing effects on time scales of a few μs. These secondary pulses are understood to be due to the creation of ions in the residual gas of the PMT which are accelerated towards the photocathode. The level of this effect was measured for just one of the PMTs (CB0274) by analysing the distribution of the time-interval between pairs of consecutive pulses. An excess rate of small interval events was observed when compared with the expected interval distribution due to Poisson statistics. Using data with the PMT both illuminated and in darkness, this excess was found to be consistent with photoelectron initiated afterpulsing at the level of $(0.7 \pm 0.1)\%$. This value was subtracted from subsequent measurements on CB0274. The correction was also applied for the other PMTs but with an estimated uncertainty of 0.5%.

3. Measurement procedure

After installation into the system, each PMT was left in the dark with high voltage applied for at least 24 h prior to measurements. This allowed the dark count to reach a low and stable level in the range 1000–1800 Hz. Tube PAVJ was somewhat noisier with a dark count that fluctuated around a mean value of 2050 Hz by up to ~ 200 Hz, a behaviour that was not apparent in the other PMTs. The reason for this phenomenon is not understood, but it is not unknown in photomultipliers.

In the event of the measuring enclosure being opened the voltage was first switched off and the PMT exposed to a minimum of room light. Before starting a sequence of measurements, a charge spectrum from the PMT was recorded with sufficient illumination for 10 000 Hz and the discriminator threshold was set for $\frac{1}{4}$ spe.

During the first stage of each run the wavelength from the monochromator was varied over the range 250–750 nm in 10 nm steps each time measuring the throughput of the system with the reference photodiode and transferring this calibration to the monitor photodiode. The sequence was then repeated for measurements of PMT efficiency at each wavelength. The neutral density filters were used to attenuate the input beam during each step in order to obtain a count rate of approximately 10 000 Hz. A sequence of measurements were made where the PMT pulses were counted for time intervals of 10 s. This was done for both source on and source off so that the dark count could be measured and subtracted. In the final stage, the reference detector was used once again while scanning over the full range of wavelengths to assess the drift in calibration during the course of the run. This can change due to heating of the integrating sphere for example.

4. Results

Fig. 5 shows the measured efficiencies for the four photomultipliers. A summary of the major uncertainties is given in Table 1, where those errors common to different wavelengths are listed separately as correlated errors. These affect the

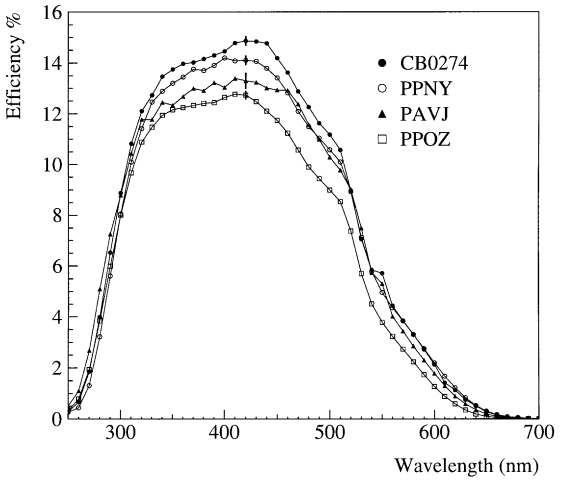

Fig. 5. The measured efficiencies of the four Hamamatsu R1408 PMTs. Error bars (1σ) are shown for 420 nm.

Table 1
Breakdown of 1σ uncertainties for the PMT measurements, expressed as a percentage of the absolute efficiency. The smaller error on afterpulsing subtraction indicated in brackets applies to tube CB0274

	250–390 nm	400–750 nm
Uncorrelated		
Scale	0.50	0.05
Spectral responsivity	0.58	0.29
System drift	1.44	0.58
Photomultiplier signal	0.20	
Correlated		
Source-reference distance		0.87
Afterpulsing subtraction		0.50(0.10)
Discriminator setting		0.30
Magnetic field correction		0.20
Source-PMT distance		0.15
Scattered light subtraction		0.05

normalization of the curve but not the shape. Scale refers to the uncertainty in the calibration of the NPL standard while spectral responsivity refers to that in the transfer of the calibration from the standard to the reference photodiode used in these measurements. System drift represents the uncertainty in the throughput of the system during a measurement. The error on the photomultiplier signal includes uncertainties from counting statistics and background subtraction. The value given in the table (0.2%) is that obtained where a high count rate was possible. Table 2 shows combined uncertainties, and the larger values at shorter wavelengths reflect poorer counting statistics.

Table 2
Total 1σ uncertainties for the PMT measurements (as percentage of efficiency). The values from Table 1 are combined in quadrature along with random errors from counting statistics

Wavelengths (nm)	Uncertainty (%)
250	5.9
260	3.1
270	2.4
280	2.4
290	2.1
300–390	2.0
400–750	1.3

The curves showing absolute efficiency have very similar shapes and differ mainly by a scaling factor. Note that the data for PAVJ shows some fluctuations which are due to its unstable dark count. For this PMT, the errors listed in Tables 1 and 2 must be combined with an additional random error at the level of 2% of the peak efficiency.

4.1. Comparison with known relative efficiencies

The relative efficiencies at 386 nm of all SNO photomultipliers have previously been measured in a testing facility at Queen's University, Kingston, Canada [8]. The data obtained for PPNY, PPOZ and PAVJ are shown in Table 3 (CB0274 was not part of the official set of SNO PMTs tested). The values given are relative to a reference PMT. Equivalent values for our data have been obtained by scaling to the same overall normalization. Given this normalization, there is good agreement between the two sets of data.

4.2. Comparison with Cherenkov source data

Boardman et al. [5] constructed a Cherenkov source based upon the encapsulation of a ^{90}Sr solution in a glass bulb. The ^{90}Sr beta decays to

Table 3
Relative efficiencies of the PMTs at 386 nm. The values for the present data have been scaled to best match the normalization of the Queen's data. Standard errors are given in brackets

	PPNY	PPOZ	PAVJ	CB0274	SNO Ave.
Queen's data	1.19(3)	1.07(3)	1.12(4)		1.10
Present data	1.187(21)	1.067(19)	1.125(30)	1.223(22)	

^{90}Y with endpoint 0.55 MeV which in turn has a $\sim 100\%$ decay branching ratio to ^{90}Zr with endpoint 2.28 MeV. Measurements of the efficiency of CB0247 were made using the source and were reported by Boardman in Ref. [6]. The count rate was related to the known source activity A, and the mean source intensity per beta decay, $(\mathrm{d}N/\mathrm{d}\omega)$, by

$$R = 2\pi\eta_c c A\Omega \int_{300\ \mathrm{nm}}^{700\ \mathrm{nm}} Q(\lambda)T(\lambda)\left(\frac{\mathrm{d}N}{\mathrm{d}\omega}\right)\frac{\mathrm{d}\lambda}{\lambda^2} \qquad (2)$$

where c is the vacuum speed of light, Ω is the fractional solid angle that was subtended at the source by the photocathode (having an exposed diameter of 186.5 ± 0.1 mm), $Q(\lambda)$ is the quantum efficiency of the PMT and $T(\lambda)$ is the transmission of an acrylic filter that was placed between the source and the PMT to provide a well-defined lower wavelength cut-off at ~ 370 nm. The photon yield, $(\mathrm{d}N/\mathrm{d}\omega)$, is not quite independent of frequency, due to the small variation in refractive index of water over the wavelength range indicated above. In practice, this effect makes a negligible difference to the comparison given below and the term is treated as a constant.

The one unknown quantity is η_c, the collection efficiency,[1] which is assumed to be independent of wavelength. In the Cherenkov source measurements, the count rate, R, was measured and the integral in Eq. (2) evaluated to determine values of η_c for various discriminator settings. It is this data which is given by Boardman [6].

[1] This includes the counting efficiency of the PMT electronics, arising from a discriminator setting at $\frac{1}{4}$ spe.

In order to determine whether our measurements are consistent with Boardman's data, we first write an expression for the count rate, R', that would be expected in the Cherenkov source measurements according to our measured efficiency, $\eta(\lambda)$, for CB0274.

$$R' = 2\pi c A\Omega k_e k_g \int_{300\ \mathrm{nm}}^{700\ \mathrm{nm}} \eta(\lambda)T(\lambda)\left(\frac{\mathrm{d}N}{\mathrm{d}\omega}\right)\frac{\mathrm{d}\lambda}{\lambda^2}. \qquad (3)$$

Two small correction factors, k_e and k_g, have been introduced. They account for the ways in which the system for the Cherenkov source measurements differed from ours both in the configuration of the electronics and the geometry, respectively.

The settings of the electronics differed because Boardman used the peak of the charge spectrum to define the "single photoelectron" charge rather than the mean which lies $\sim 50\%$ higher for CB0274. As the spe charge is used to establish a gain of 10^7, the PMT voltage must be set higher in the first case. This will lead to a small increase in efficiency, but the most important difference is that the fraction of the charge spectrum falling above the $\frac{1}{4}$ spe discriminator level is $\sim 5\%$ greater when spe refers to the peak. The correction factor was determined using an uncalibrated Cherenkov source by simply measuring the relative efficiency at the two gain/discriminator settings, giving $k_e = 1.066 \pm 0.006$.

The geometry differed in that the Cherenkov source was placed slightly further from the PMT (at 1.5 m) and a smaller area of PMT was exposed (10% less). It is the effect of the latter which dominates as the efficiency of the outer 10% is lower, due to greater angles of incidence on the PMT glass bulb and a consequent higher probability of

reflection. The factor k_g was estimated to be 1.011 ± 0.003 based on a model of the PMT optics.

The Cherenkov source data may now be compared with our measurements by considering the ratio R'/R which may be obtained from Eqs. (3) and (2) using our data and that given in Ref. [6]:

$$\frac{R'}{R} = 1.091 \pm 0.041. \quad (4)$$

The error includes systematic errors in $\eta(\lambda)$ and η_c, but is dominated by a 3.5% contribution for the intensity of the Cherenkov source.

While this 2.2σ deviation from unity just might be statistical, it might also suggest a problem with one of the measurements. Many small corrections have gone into the calculation of the Cherenkov source intensity, and in the comparison with our data. There are two effects which could account for the difference and which are not discussed in Ref. [5]:

(1) A reduction in the observed rate from the Cherenkov source is expected due to photon coincidences. As the light is emitted from the source in short bursts following each decay, it is possible for multiple photons from a single decay to strike the PMT and give photoelectrons, but only give rise to a single count. The effect will be dominated by higher yield decays since the coincidence probability increases with photon yield, and such decays contribute most to the intensity of the source. In addition, the distribution of Cherenkov light from a charged particle is not isotropic and this enhances the probability of coincidence. A simulation of the source with SNO simulation code shows that any Cherenkov photon detected by the PMT will, on average, be accompanied by 0.44 other photons from the same decay which can strike the PMT (in the wavelength range 370–720 nm). With the acrylic filter in place, the average detection efficiency in the range is 8.4%, leading to an observed rate of detected photons 3.7% lower than the true rate.

(2) Light can be trapped in the source by total internal reflection at the outer glass–air boundary of the bulb if the angle of incidence exceeds 42°. As the source is spherically symmetric, such photons continue to reflect off the outer surface until they are either scattered or absorbed. The glass bulb has an outer diameter of 51 mm and a wall thickness of 5 mm, so the 42° translates to an incident angle of $\theta_w = 68°$ on the inner water–glass boundary. For light generated uniformly throughout the solution and isotropic in direction, the fraction trapped is given by $\cos^3 \theta_w \simeq 5\%$. Light generated within the glass contributes only $\sim 6\%$ of the total yield but has a 65% probability of being trapped assuming that it is generated isotropically. The result of these effects is a reduction of the light output at the level of a few percent, but little more can be said without additional information on the relative amount of scattering and absorption within the source.

4.3. Comparison with quantum efficiency data

If the collection efficiency η_c were independent of wavelength then the absolute efficiency for single-photon counting as a function of wavelength would be expected to match the shape of measured quantum efficiency curves (made with the PMT wired up as a diode so that the collection efficiency is effectively equal to one). Quantum efficiency curves are shown in Fig. 6 for two R1408 PMTs made before the production run for testing purposes. They are shown together with the average of our efficiency data for all four PMTs measured and have been scaled to have the same overall normalization. It can be seen that the points corresponding to our data lie closely to one of the curves, but not the other which shows a relatively low response at long wavelengths. This could well be explained by tube to tube variations in the photocathode although the absolute efficiency curves in Fig. 5 show somewhat less variation between PMTs.

Without scaling, the peak quantum efficiency of the pre-production PMTs is $\sim 21.7\%$. A similar value for our four calibrated PMTs would imply a combined collection and counting efficiency of $\sim 62\%$.

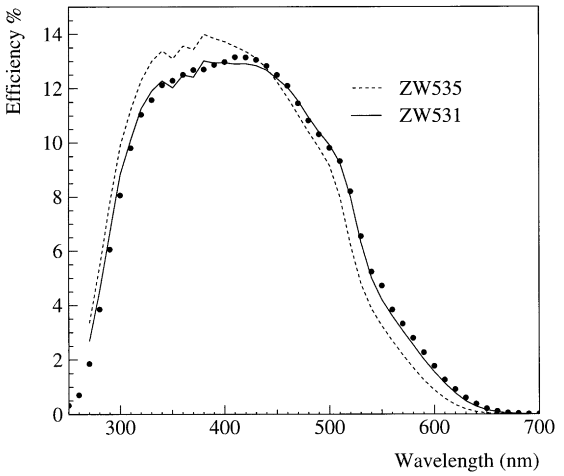

Fig. 6. Comparison of the average efficiency for the four measured PMTs with curves for the quantum efficiency of two similar R1408 PMTs (ZW531, ZW535). These have been scaled to the same normalization as our data to show the difference in shape.

Acknowledgements

The authors would like to thank the UK Particle Physics and Astronomy Research Council for the provision of funding for this project.

References

[1] G.T. Ewan, Nucl. Instr. and Meth. A 314 (1992) 373.
[2] G. Doucas et al., Nucl. Instr. and Meth. A 370 (1996) 579.
[3] M.D. Lay, Nucl. Instr. and Meth. A 383 (1996) 485.
[4] M.D. Lay, M.J. Lyon, Nucl. Instr. and Meth. A 383 (1996) 495.
[5] R.J. Boardman et al., Nucl. Instr. and Meth. A 345 (1994) 356.
[6] R.J. Boardman, D.Phil. Thesis, Oxford, 1992.
[7] Fu Lei, J. Fischer, Metrologia 30 (1993) 297.
[8] C.J. Jillings et al., Nucl. Instr. and Meth. A 373 (1996) 421.
[9] N.P. Fox, E. Theocharons, T.H. Ward, Metrologia 35 (1998) 535.